# Purified and synthetic Alzheimer's amyloid beta (Aβ) prions

Jan Stöhr[a,1], Joel C. Watts[a,1], Zachary L. Mensinger[a,b], Abby Oehler[c], Sunny K. Grillo[a], Stephen J. DeArmond[a,c], Stanley B. Prusiner[a,d,2], and Kurt Giles[a,d]

[a]Institute for Neurodegenerative Diseases and Departments of [c]Pathology and [d]Neurology, University of California, San Francisco, CA 94143; and [b]Department of Chemistry, University of California, Berkeley, CA 94720

Contributed by Stanley B. Prusiner, April 24, 2012 (sent for review March 15, 2012)

**The aggregation and deposition of amyloid-β (Aβ) peptides are believed to be central events in the pathogenesis of Alzheimer's disease (AD). Inoculation of brain homogenates containing Aβ aggregates into susceptible transgenic mice accelerated Aβ deposition, suggesting that Aβ aggregates are capable of self-propagation and hence might be prions. Recently, we demonstrated that Aβ deposition can be monitored in live mice using bioluminescence imaging (BLI). Here, we use BLI to probe the ability of Aβ aggregates to self-propagate following inoculation into bigenic mice. We report compelling evidence that Aβ aggregates are prions by demonstrating widespread cerebral β-amyloidosis induced by inoculation of either purified Aβ aggregates derived from brain or aggregates composed of synthetic Aβ. Although synthetic Aβ aggregates were sufficient to induce Aβ deposition in vivo, they exhibited lower specific biological activity compared with brain-derived Aβ aggregates. Our results create an experimental paradigm that should lead to identification of self-propagating Aβ conformations, which could represent novel targets for interrupting the spread of Aβ deposition in AD patients.**

neurodegenerative | APP23 | proteinopathies | luciferase | glial fibrillary acidic protein

Alzheimer's disease (AD) is a neurodegenerative disorder characterized by behavioral changes and the progressive loss of cognitive function. The brains of AD patients contain extracellular amyloid plaques composed of amyloid-β (Aβ) peptides as well as intracellular neurofibrillary tangles containing hyperphosphorylated tau protein. The amyloid cascade theory postulates that aggregation of Aβ peptides cleaved from the amyloid precursor protein (APP) and the subsequent spread of Aβ deposits in the brain constitute the earliest key events in the progression of AD (1, 2). Transgenic (Tg) mice expressing mutant human APP linked to familial AD develop age-related Aβ deposits in the brain and are widely used as models of cerebral β-amyloidosis (3–6).

Recent experimental data have shown that Aβ amyloid-laden brain homogenates induce Aβ deposition in Tg mice expressing mutant human APP (7–10) as well as in Tg mice expressing wild-type (WT) human APP and Tg rats expressing mutant human APP that do not develop Aβ deposits spontaneously (11, 12). This seeded deposition is reminiscent of mammalian prion diseases in which $PrP^{Sc}$, a misfolded and infectious conformer of the prion protein (PrP), self-propagates by inducing the misfolding of cellular PrP, ultimately leading to aggregation and neurodegeneration (13). More generally, prions are defined as alternatively folded, self-propagating protein conformers. Self-perpetuating protein isoforms participate in diverse biological processes including translation termination, long-term memory storage, and the immune response, suggesting that formation of prions may be far more common than previously appreciated (14–17).

A growing body of evidence argues that self-propagating protein aggregates play central roles in many human neurodegenerative illnesses including Parkinson's disease and AD (18). In AD patients, Aβ deposits are believed to spread progressively throughout the brain (2), arguing for a prion-based mechanism of propagation. Furthermore, individuals with mutations in APP that cause early-onset AD do not typically develop disease until in their 50s, despite the presence of the mutation from birth, suggesting that formation of Aβ prions is required to initiate disease. Thus, targeting the formation of Aβ prions in the brain may constitute an ideal therapeutic strategy for treating AD during its earliest stages.

There is currently no direct evidence for the existence of Aβ prions, defined as Aβ assemblies capable of self-propagation within the brain. Definitive proof would require formation of a self-propagating protein aggregate in the absence of additional cofactors, as has been shown for several prions including those composed of PrP, Sup35, and HET-s (19–22). Previous attempts to initiate Aβ aggregation in vivo with synthetic Aβ peptides were not successful within the time frame analyzed (8), raising the possibility that auxiliary factors may be necessary for conversion to the prion state. Here, we demonstrate that widespread cerebral Aβ deposition is induced following inoculation of Tg mice with purified brain-derived Aβ fibrils as well as aggregates composed of synthetic Aβ peptides. Although synthetic Aβ preparations exhibited lower specific bioactivity than Aβ aggregates derived from the brain, these results provide compelling evidence that Aβ aggregates are prions and that Aβ alone is sufficient for the formation of a self-propagating protein assembly.

## Results

The kinetics of spontaneous and induced Aβ deposition can be monitored in live mice using bioluminescence imaging (BLI) (10). When mice expressing a luciferase (luc) reporter under the control of the glial fibrillary acidic protein (*Gfap*) promoter (23) were crossed with Tg mice expressing human APP with the Swedish double mutation (5), the resulting bigenic Tg(APP23:*Gfap*-luc) mice showed an increase in the bioluminescence signal in their brains beginning at 416 ± 9 d of age, concomitant with spontaneous Aβ deposition (Table S1). To determine whether Aβ deposition could be accelerated in these animals in a prion-like fashion, Tg(APP23:*Gfap*-luc) mice were intracerebrally (ic) inoculated in the right cerebral hemisphere with brain homogenates from either aged Tg(APP23) or Tg(CRND8) mice, the latter express mutant human APP with both the Swedish and Indiana mutations (6). The brain homogenates prepared from aged Tg(APP23) and Tg(CRND8) mice produced a sustained increase in the brain BLI signal of bigenic mice at 261 ± 8 and 238 ± 12 d postinoculation (dpi), respectively (Fig. 1*A* and Table

Author contributions: J.S., J.C.W., S.B.P., and K.G. designed research; J.S., J.C.W., Z.L.M., A.O., and S.K.G. performed research; J.S., J.C.W., S.J.D., S.B.P., and K.G. analyzed data; and J.S., J.C.W., S.B.P., and K.G. wrote the paper.

The authors declare no conflict of interest.

[1]J.S. and J.C.W. contributed equally to this work.

[2]To whom correspondence should be addressed. E-mail: stanley@ind.ucsf.edu.

This article contains supporting information online at www.pnas.org/lookup/suppl/doi:10.1073/pnas.1206555109/-/DCSupplemental.

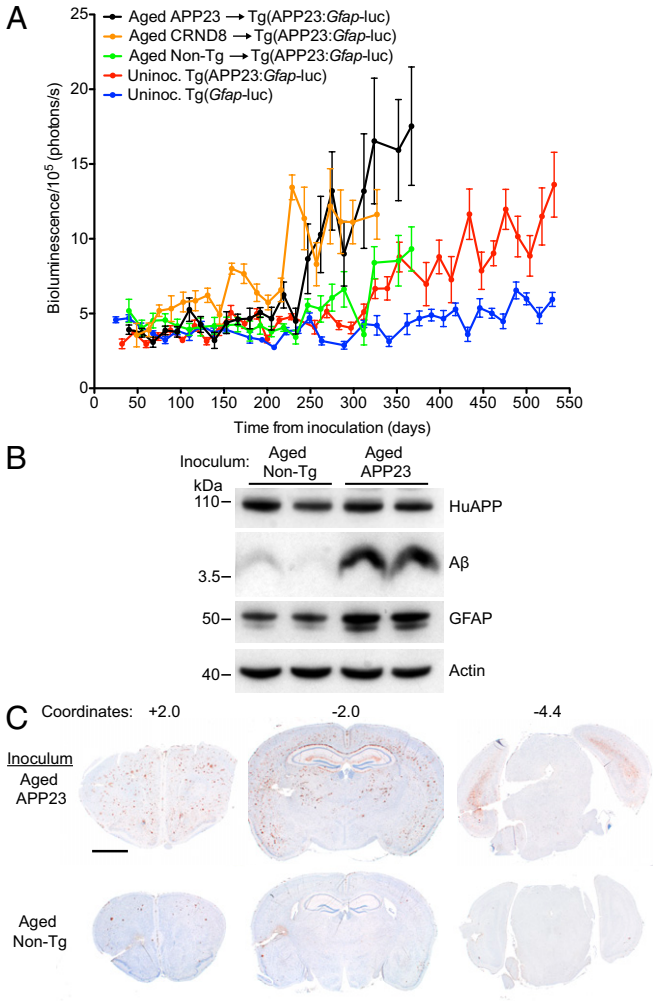


**Fig. 1.** Induction of widespread Aβ deposition in Tg(APP23:*Gfap*-luc) mice inoculated with Aβ amyloid-laden brain homogenate. (*A*) Mean brain bioluminescence (± SEM) signals obtained from uninoculated Tg(*Gfap*-luc) mice (blue, $n = 16$), uninoculated Tg(APP23:*Gfap*-luc) mice (red, $n = 12$), Tg(APP23:*Gfap*-luc) mice inoculated with aged non-Tg brain homogenate (green, $n = 6$), and Tg(APP23:*Gfap*-luc) mice inoculated with aged Tg(APP23) (black, $n = 6$) or Tg(CRND8) (orange, $n = 12$) brain homogenate. An accelerated increase in the brain BLI signal was observed in mice inoculated with aged Tg(APP23) and Tg(CRND8) brain homogenate compared with mice inoculated with non-Tg brain homogenate and age-matched uninoculated mice. (*B*) By immunoblotting, increased GFAP and total Aβ levels were apparent in brain homogenates prepared from male Tg(APP23)-inoculated Tg(APP23:*Gfap*-luc) mice at 385 dpi compared with age-matched mice inoculated with non-Tg brain homogenate. Actin is shown as a control. (*C*) Widespread induction of Aβ deposition in female Tg(APP23:*Gfap*-luc) mice inoculated with aged Tg (APP23) brain homogenate at 330 dpi compared with age-matched mice inoculated with brain homogenate from non-Tg mice. Coronal brain sections, cut at the indicated rostral–caudal stereotaxic coordinates, were stained with an anti-Aβ antibody. (Scale bar, 2 mm.)

S1), whereas the BLI signal remained low in Tg(APP23:*Gfap*-luc) mice inoculated with aged non-Tg brain homogenate until it increased at 333 ± 9 dpi. Statistical analyses showed no significant difference between the ages at which the BLI signal increased in the uninoculated mice (416 ± 9 d) and those inoculated with aged non-Tg brains (393 ± 9 d) (Table S1). At 385 dpi, levels of Aβ and GFAP in the brains of bigenic mice were substantially higher in those inoculated with aged Tg(APP23) brain homogenate than those receiving the control aged non-Tg homogenate (Fig. 1*B*). In mice inoculated with aged Tg(APP23) brain homogenate, Aβ deposition was elevated throughout the cortical layers of the forebrain at 330 dpi compared with mice inoculated with aged non-Tg brain homogenate (Fig. 1*C*), similar to the widespread Aβ deposition observed in Tg(APP23)-inoculated R1.40 Tg mice (24). Interestingly, despite unilateral inoculation, the pathology was bilateral, arguing for the progressive spread of Aβ deposition throughout the brain. Cumulatively, these results demonstrate that widespread Aβ deposition can be induced in the brains of Tg (APP23:*Gfap*-luc) mice by inoculation with brain homogenate containing Aβ aggregates.

We next sought more direct evidence for the existence of Aβ prions. Using a purification protocol for amyloid aggregates that employs limited digestion with proteinase K (PK) (25), Aβ aggregates were purified from brain homogenates of aged Tg (APP23) and Tg(CRND8) mice. Purification of Aβ from either line routinely produced fractions enriched for Aβ as detected by silver staining (Fig. 2*A*). Transmission electron microscopy identified the predominant aggregates as fibrils, which were mostly bundled together in dense arrays (Fig. 2*B*). Purified Aβ fractions from Tg(APP23) and Tg(CRND8) mice contained ∼15–20-fold more Aβ than crude brain homogenate (Table S2) and produced an increase in the BLI signal at 161 ± 7 and 173 ± 9 dpi, respectively (Table S1 and Fig. 2*C*). Immunoblots and ELISAs revealed high levels of Aβ(1–40), Aβ(1–42), and GFAP in the brains of mice inoculated with Aβ purified from the brains of either Tg(APP23) or Tg(CRND8) mice at 300 dpi compared with age-matched, uninoculated animals (Fig. 2 *D* and *E*). Aβ deposition in Tg(APP23:*Gfap*-luc) mice inoculated with Aβ purified from Tg(APP23) (Fig. 2 *F–I*) or from Tg(CRND8) mice (Fig. S1) was widespread and prominent throughout the brain compared with control animals (Fig. 2 *J–M*). Our results argue that purified Aβ preparations are sufficient to induce widespread Aβ deposition in vivo, providing compelling evidence for the existence of Aβ prions.

Although Aβ fibrils purified from the brain induced Aβ deposition, we could not exclude the copurification of other cofactors essential for the observed prion behavior of Aβ. We therefore sought to induce Aβ deposition in vivo using preparations of Aβ aggregates composed of synthetic Aβ peptides. For these studies, we used WT Aβ(1–40) and a mutant Aβ(1–40) peptide containing cysteine at position 26, enabling the formation of covalent dimers, denoted $(AβS26C)_2$, which was reported to inhibit efficiently long-term potentiation and form stable neurotoxic protofibrils (26, 27). These two peptides were solubilized in ammonium bicarbonate/sodium phosphate buffer and then incubated at 37 °C for 72 h to induce amyloid formation as demonstrated by elevated thioflavin T (ThioT) fluorescence. Distinct polymerization kinetics and ThioT fluorescence for the two synthetic Aβ peptides suggested different tertiary and quaternary structures (Fig. 3*A*). Synthetic Aβ aggregates were digested by proteinase K, whereas brain-derived Aβ aggregates were largely protease resistant (Fig. S2). Undigested Aβ(1–40) migrated as a monomer in SDS/PAGE, and $(AβS26C)_2$ was largely dimeric (Fig. S2). Electron microscopy and atomic force microscopy revealed that both preparations contained fibrillar and globular structures (Fig. 3*B*). Fibrils composed of Aβ(1–40) were longer than those containing $(AβS26C)_2$, which presumably reflects different aggregate structures.

Synthetic Aβ aggregates composed of either WT Aβ(1–40) or $(AβS26C)_2$ were ic inoculated into young Tg(APP23:*Gfap*-luc) mice at a concentration of 250 μg/mL, ∼100-fold higher than the Aβ in brain homogenates (Table S2). Both synthetic Aβ(1–40) and $(AβS26C)_2$ preparations produced elevated BLI signals at 229 ± 5 and 234 ± 9 dpi, respectively (Fig. 3*C* and Table S1). Brains from Tg(APP23:*Gfap*-luc) mice inoculated with either synthetic Aβ(1–40) or $(AβS26C)_2$ aggregates at 330 dpi contained higher levels of Aβ and GFAP compared with age-matched uninoculated animals,

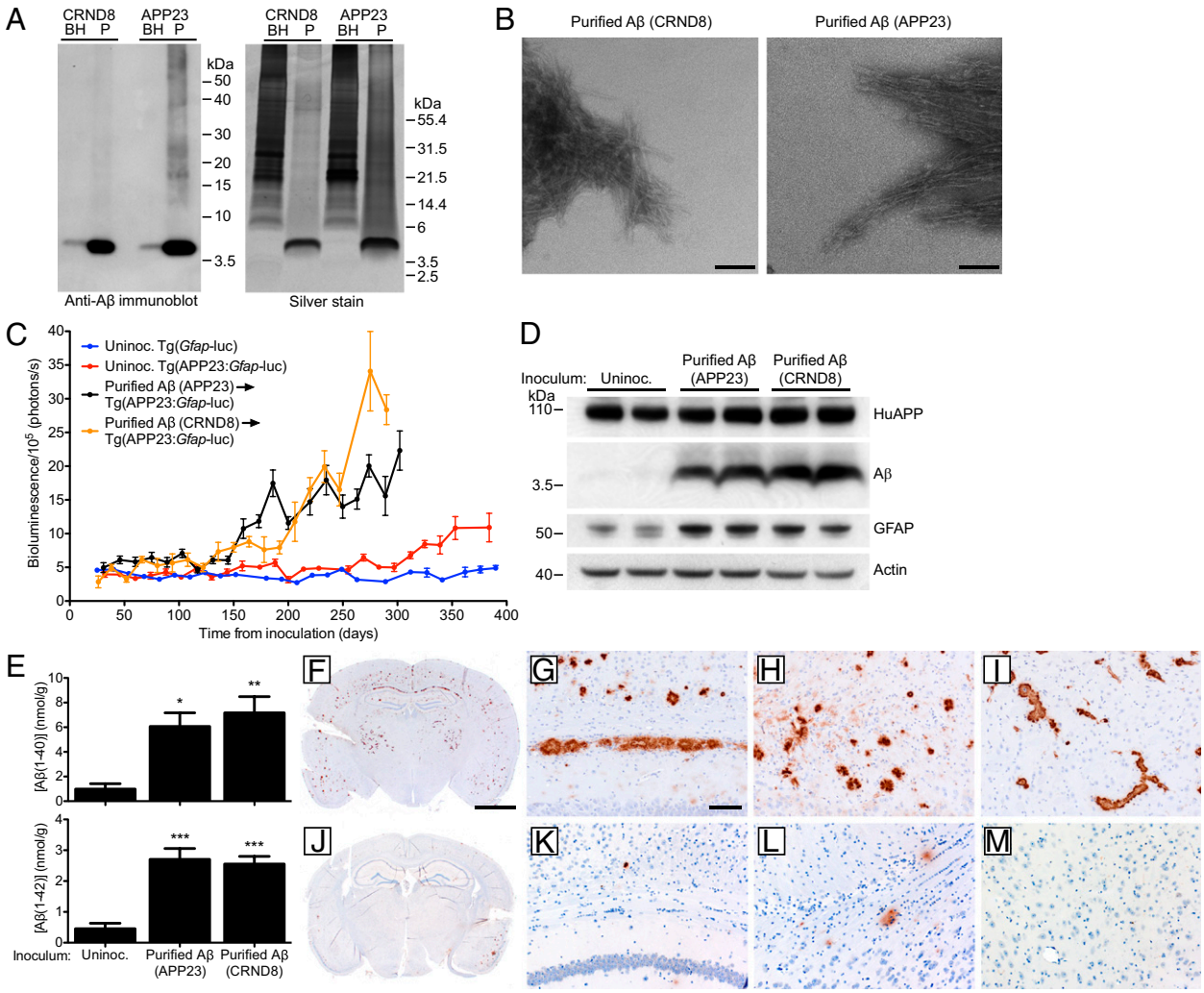


**Fig. 2.** Induction of Aβ deposition in Tg(APP23:*Gfap*-luc) mice inoculated with purified brain-derived Aβ fibrils. (*A*) Aβ immunoblot (*Left*) and silver staining (*Right*) of unpurified brain homogenates (BH) and purified Aβ aggregates (P) from aged Tg(CRND8) and Tg(APP23) mice demonstrated that Aβ peptides are the major protein species after purification. (*B*) Electron microscopy of purified Aβ fibrils from aged Tg(CRND8) (*Left*) and Tg(APP23) mice (*Right*) confirmed the isolation of intact Aβ fibrils. (Scale bars, 100 nm.) (*C*) Mean brain bioluminescence (± SEM) signals obtained from uninoculated Tg(*Gfap*-luc) mice (blue, $n$ = 16), uninoculated female Tg(APP23:*Gfap*-luc) mice (red, $n$ = 6), and female Tg(APP23:*Gfap*-luc) mice inoculated with Aβ fibrils purified from either aged Tg (APP23) brains (black, $n$ = 11) or aged Tg(CRND8) brains (orange, $n$ = 9). Increased BLI signals were observed in mice inoculated with the purified Aβ fibrils by ~160 dpi . (*D*) By immunoblotting, increased GFAP and Aβ protein levels were apparent in brain homogenates prepared from female Tg(APP23:*Gfap*-luc) mice inoculated with Aβ fibrils purified from aged Tg(APP23) or Tg(CRND8) mice at 300 dpi compared with age-matched, uninoculated mice. Actin levels are shown as a control. (*E*) By ELISA, Aβ(1–40) (*Upper*) and Aβ(1–42) (*Lower*) levels were significantly increased in Tg(APP23:*Gfap*-luc) mice inoculated with purified Aβ fibrils from Tg(APP23) or Tg(CRND8) mice at 300 dpi compared with age-matched, uninoculated controls ($n$ = 4 each). $^{*}P < 0.05$, $^{**}P < 0.01$, $^{***}P < 0.001$. Data are mean ± SEM. (*F–M*) Aβ immunostaining of brain sections from female Tg(APP23:*Gfap*-luc) mice inoculated with purified Tg(APP23) Aβ fibrils (*F–I*) or aged non-Tg brain homogenate (*J–M*) at 300 dpi. Increased Aβ deposition was apparent in whole brain coronal sections (*F* and *J*) as well as the hippocampus and overlying cortex (*G* and *K*), entorhinal cortex (*H* and *L*), and thalamus (*I* and *M*) of Aβ-inoculated mice compared with mice inoculated with non-Tg brain homogenate. (Scale bar in *F*, 2 mm and also applies to *J*; scale bar in *G*, 100 μm and also applies to *H*, *I*, and *K–M*.)

as determined by immunoblotting (Fig. 4*A*). Compared with uninoculated animals, Aβ(1–40) and Aβ(1–42) levels were increased ~5- and 4-fold, respectively, in mice inoculated with synthetic Aβ aggregates (Fig. 4*B*). The mice inoculated with synthetic Aβ peptides exhibited Aβ deposits primarily in the subcallosal region of the hippocampus and in the thalamus (Fig. 4 *C–H*). These Aβ deposits bound thioflavin S (Fig. S3) and were accompanied by an increase in GFAP staining (Fig. S4). Similar to Aβ deposits induced by brain-derived Aβ aggregates, the neuropathology was bilateral (Fig. 4 *C* and *F*). These cerebral Aβ deposits could not be due to residual peptide from the inoculated synthetic Aβ because Aβ deposition could not be detected by immunoblotting or immunohistochemistry between 33 and 83 dpi (Fig. S5).

## Discussion

In the studies reported here, Aβ aggregates either purified from the brains of Tg mice expressing mutant APP or composed of synthetic peptides induced widespread cerebral Aβ amyloidosis following ic inoculation into Tg(APP23:*Gfap*-luc) mice. Our results provide incontrovertible evidence that Aβ aggregates are prions and that the formation of Aβ prions does not require additional proteins or cofactors.

BLI can be used to monitor the kinetics of both Aβ and PrP prion replication in living mice: as each of these prions accumulates, they stimulate astrocytic gliosis, which results in up-regulation of the *Gfap* promoter (Fig. 1) (10, 28). Using BLI, we assigned incubation times by measuring the time from inoculation to the

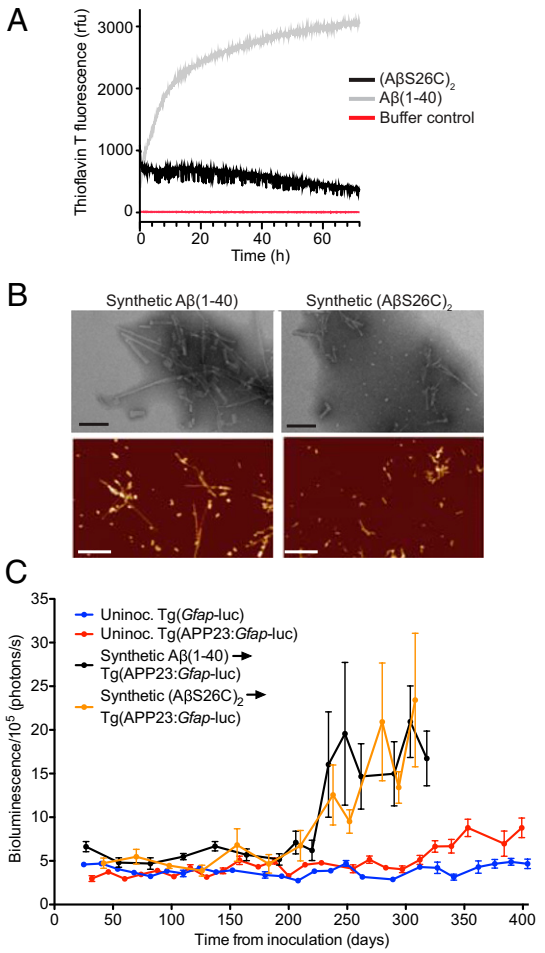


**Fig. 3.** Formation and characterization of synthetic Aβ prions. (*A*) Time course of thioflavin T measurements of Aβ(1–40) (gray line) and $(A\beta S26C)_2$ (black line) following solubilization, compared with buffer control (red line). (*B*) Electron microscopy (*Upper*) (Scale bars, 100 nm.) and atomic force microscopy images (*Lower*) (Scale bars, 500 nm) of fibrillar aggregates from Aβ (1–40) and $(A\beta S26C)_2$. (*C*) Mean brain bioluminescence (± SEM) signals obtained from uninoculated Tg(*Gfap*-luc) mice (blue, $n = 16$), uninoculated Tg (APP23:*Gfap*-luc) mice (red, $n = 12$), and Tg(APP23:*Gfap*-luc) mice inoculated with synthetic Aβ aggregates composed of either WT Aβ(1–40) peptide (black, $n = 6$) or $(A\beta S26C)_2$ peptide (orange, $n = 8$). An increase in the BLI signal was observed in mice inoculated with the synthetic Aβ aggregates by ~230 dpi.

beginning of a sustained increase in the brain bioluminescence signal. When the Aβ aggregates were purified from the brains of either Tg(APP23) or Tg(CRND8) mice and bioassayed in Tg(APP23:*Gfap*-luc) mice, changes in the BLI signal were detected at 161 and 173 d after inoculation, respectively (Table S1 and Fig. 2). These increases in the BLI signal occurred 100 and 65 d earlier than in bigenic mice inoculated with the respective crude brain homogenates (Fig. 1 and Table S1). Notably, the purified samples had a concentration of Aβ that was ~15-fold higher than that found in the brain homogenates (Table S2). The ~40% reduction in the incubation period argues that the purified samples contain substantially more bioactive Aβ than the homogenates (Figs. 1 and 2). With PrP prions, there is an inverse relationship between the dose of prions in the inoculum and the length of the incubation time (29); it seems likely that a similar relationship will be found with Aβ prions. Despite ~10-fold more Aβ in the synthetic peptide preparations compared with the purified samples, the incubation times for the synthetic Aβ aggregates in Tg(APP23:*Gfap*-luc) were longer (Table S1). Moreover, the bigenic mice inoculated with synthetic Aβ showed somewhat less Aβ deposition compared with those receiving purified brain-derived Aβ aggregates (Figs. 2 and 4).

The properties of the Aβ prions in the purified preparations resembled those found in the crude homogenates, which include aggregation, reactivity with anti-Aβ antibodies, protease resistance, and stimulation of *Gfap*-luciferase expression and Aβ deposition. The protease resistance of the Aβ prions resembles $PrP^{Sc}$ in that both were resistant to digestion by PK. Interestingly, all of the induced Aβ deposits were largely PK resistant, regardless of the degree of protease resistance of the Aβ species present in the inoculum (Fig. S2). Whereas PK-resistant Aβ amyloid fibrils were sufficient to induce Aβ deposition in vivo, other Aβ assemblies, including more soluble Aβ species (30), may also exhibit prion-like behavior.

The incubation periods for our synthetic Aβ prions were similar to those for the crude brain homogenates (Table S1) although the synthetic Aβ inocula contained ~100-fold more Aβ peptide than the brain homogenates (Table S2). This finding is analogous to our initial preparations of synthetic PrP prions, for which extended incubation periods are thought to derive from a structural disparity between amyloid fibrils composed of recombinant PrP (recPrP) and $PrP^{Sc}$ purified from infected brain (22, 31, 32). One possible explanation for the different bioactivity observed for synthetic and brain-derived Aβ aggregates is that only a subset of the synthetic Aβ aggregates are able to initiate template-based propagation. Alternatively, the synthetic Aβ aggregates constitute a distinct Aβ conformation or "strain" that propagates more slowly. Indeed, multiple distinct, polymeric Aβ structures can be generated spontaneously (33, 34) or by seeding with naturally occurring Aβ aggregates (35). This highlights the need for caution in interpreting current structural models of Aβ fibrils formed from synthetic peptides (35, 36) and suggests that such preparations need to be monitored by bioassay.

The high concentration of Aβ peptide in our synthetic Aβ prion preparations raised the issue of how much of the Aβ detected in mouse brains after the rise in BLI signal was due to residual Aβ from the inoculum. The absence of detectable Aβ in brain sections or homogenates prepared from mice between 33 and 83 dpi argues that residual Aβ peptides from the inocula are below the level of detection (Fig. S5). Similarly, no Aβ deposition was found at 1 mo postinoculation in Tg(APP23) mice inoculated with aged Tg(APP23) brain homogenate (8). In addition, over 95% of the ic-inoculated synthetic Aβ peptide is likely to have been rapidly cleared from the brain; this phenomenon has been observed with both bacteriophage and $PrP^{Sc}$ (37, 38).

In contrast to PrP prions, the replication of Aβ prions seems considerably less robust. Moreover, Tg(APP23) mice expressing mutant human APP are required to detect the Aβ prions; WT mice cannot be used. Nevertheless, we were able to generate biologically active, synthetic Aβ prions and thus demonstrate that Aβ alone is sufficient for the formation of Aβ prions, analogous to synthetic prions composed solely of recPrP (22, 32). Following unilateral inoculation with either synthetic or brain-derived Aβ prions, widespread induced Aβ deposition was observed throughout both hemispheres of the brain, including regions distal to the inoculation site. This suggests that Aβ prions spread throughout the brain in a manner analogous to PrP prions. Indeed, spread of Aβ aggregates along transsynaptic networks has been observed both in Tg mice and AD patients (2, 39), indicating that this phenomenon is unlikely to be an artifact of ic inoculation. Because Aβ deposition is thought to precede neurofibrillary tangle formation in AD, we hypothesize that formation and spreading of Aβ prions represents one of the earliest events in AD (2, 40).

Recent transmission studies in cellular and mouse models of neurodegenerative diseases including the tauopathies, synucleinopathies, and amyotrophic lateral sclerosis (ALS) indicate that these diseases are also caused by self-propagating protein aggregates, i.e., prions (41–47). Thus, determining the molecular

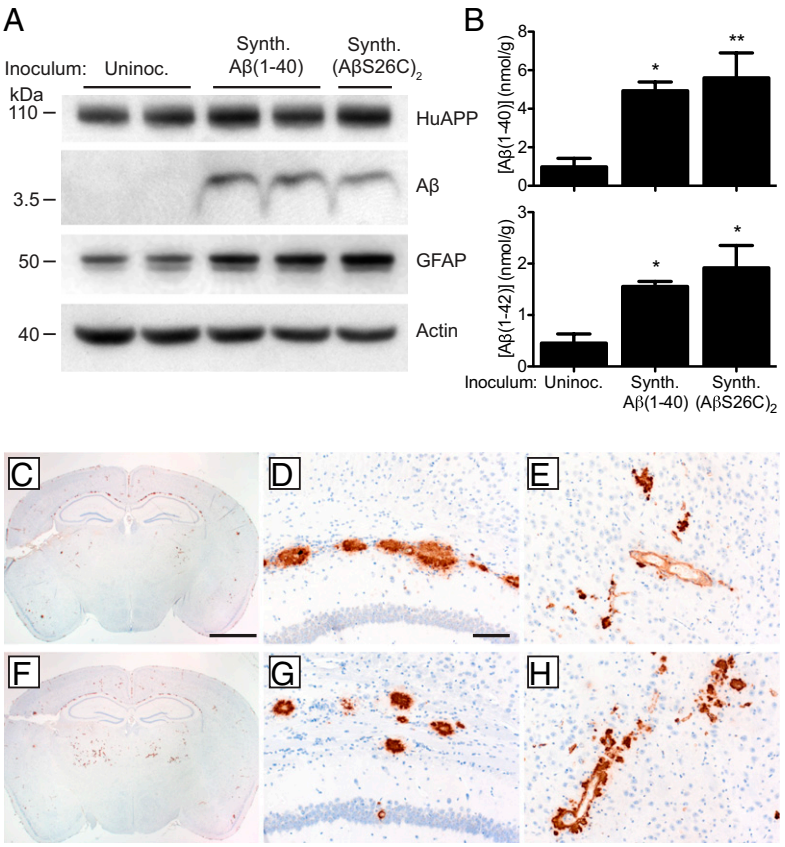


**Fig. 4.** Induction of cerebral Aβ deposition in Tg(APP23:*Gfap*-luc) mice inoculated with synthetic Aβ aggregates. (*A*) Immunoblotting shows that increased GFAP and Aβ protein levels were apparent in brain homogenates prepared from male Tg(APP23:*Gfap*-luc) mice inoculated with synthetic Aβ aggregates at 330 dpi compared with age-matched, uninoculated Tg(APP23) mice. Actin levels are shown as a control. (*B*) By ELISA, Aβ(1–40) (*Upper*) and Aβ(1–42) (*Lower*) levels were significantly increased in Tg(APP23:*Gfap*-luc) mice inoculated with synthetic Aβ(1–40) or $(AβS26C)_2$ aggregates at 330 dpi compared with age-matched, uninoculated controls ($n = 4$ each). $^*P < 0.05$, $^{**}P < 0.01$. Data are mean ± SEM (*C–H*) Aβ immunostaining of brain sections from female Tg(APP23:*Gfap*-luc) mice inoculated with synthetic Aβ(1–40) (*C–E*) or $(AβS26C)_2$ (*F–H*) aggregates at 330 dpi. Induced Aβ deposition was apparent in whole brain coronal sections (*C* and *F*) as well as the corpus callosum (*D* and *G*) and thalamus (*E* and *H*) of inoculated mice. (Scale bar in *C*, 2 mm and also applies to *F*; scale bar in *D*, 100 μm and also applies to *E*, *G*, and *H*.)

mechanisms governing prion formation and self-propagation in the brain may advance our understanding of the etiology and pathogenesis of neurodegeneration as well as facilitate identification of therapeutic targets, through which effective interventions can be developed.

Although Aβ aggregates clearly behave like prions at the molecular level, there is currently no evidence that AD is infectious in the sense that it is communicable among humans. However, cerebral Aβ deposition in mice can be initiated by injection of Aβ aggregates into the periphery (48). Whereas immunization with synthetic Aβ peptide reduced cerebral Aβ deposition and improved cognition in Tg mouse models of AD (49, 50), the long-term effects of peripheral Aβ administration are unknown. In humans, a clinical trial of Aβ immunization was halted after some patients developed meningoencephalitis (51, 52). Because our results illustrate that synthetic Aβ is capable of forming prions, individuals who have been injected with synthetic Aβ peptides may be at increased risk for cerebral Aβ deposition.

## Materials and Methods

Additional methods are provided in *SI Materials and Methods*.

**Mice.** Tg(APP23) mice expressing Swedish mutant human APP (751-amino-acid isoform) under the control of the *Thy-1.2* promoter (5) were a gift from Matthias Staufenbiel (Novartis, Basel, Switzerland) and were maintained on a C57BL/6 background. Tg(*Gfap*-luc) mice expressing firefly luciferase under the control of the murine *Gfap* promoter (23) were a gift from Caliper Life Sciences, and were maintained on an FVB/N background. Homozygous Tg(*Gfap*-luc) mice were generated by intercrossing hemizygous animals and were confirmed by backcrossing. To create bigenic mice, Tg(APP23) mice were crossed with homozygous Tg(*Gfap*-luc) animals. Tg(CRND8) mice, expressing Swedish and Indiana mutant human APP (695-amino-acid isoform) under the control of the *Prnp* promoter (6), were a gift from Paul Fraser (Centre for Research in Neurodegenerative Diseases, Toronto, Canada), and were maintained on a mixed C3H/C57BL/6 background. In all BLI experiments, equal numbers of male and female mice were used, except the experiments involving purified brain-derived Aβ fibrils, in which only female animals were used. All animal experiments were performed under protocols approved by the institutional animal care and use committee at the University of California San Francisco.

**Preparation of Synthetic Aβ Aggregates.** Wild-type Aβ(1–40) peptide was purchased from Sigma-Aldrich and the dimeric $(AβS26C)_2$ peptide from Anaspec. Lyophilized peptides were dissolved to 500 μg/mL in 25 mM ammonium bicarbonate buffer, pH 8.5. This solution was immediately diluted 1:1 in sodium phosphate buffer, pH 7.2, and 900-μL aliquots were incubated at 37 °C for 72 h in siliconized, 1.5-mL centrifugation tubes under constant agitation at 900 rpm. The resulting samples were further analyzed or snap frozen in liquid nitrogen and stored at −80 °C before inoculation.

**Mouse Inoculations.** Brain homogenates from aged Tg(APP23) mice, aged Tg(CRND8) mice, or aged non-Tg FVB mice [10% (wt/vol) in calcium- and magnesium-free PBS] were prepared using an Omni Tip (Omni International) with a Fisher Scientific PowerGen homogenizer (Fisher Scientific). Before inoculation, brain homogenates were diluted to 1% (wt/vol) in 5% BSA. For inoculations, 30 μL of 1% (wt/vol) brain homogenates, purified brain-derived Aβ aggregates, or synthetic Aβ aggregates were used. Weanling (~2-mo-old) Tg(APP23:*Gfap*-luc) mice were inoculated in the right cerebral hemisphere using a 27-gauge syringe, a method commonly used to deliver PrP prions (32).

Mice were euthanized at 300–330 dpi for injections of purified and synthetic Aβ aggregates, or 330–390 dpi for inoculations with brain homogenates.

**ACKNOWLEDGMENTS.** We thank the staff at the Hunter's Point animal facility for their assistance with the animal experiments and Marta Gavidia for mouse genotyping. The Tg(*Gfap*-luc) mice were a generous gift from Caliper Life Sciences. This work was supported by National Institutes of Health Grants AG02132, AG10770, AG021601, AG031220, and NS041997 as well as by gifts from the G. Harold and Leila Y. Mathers Charitable Foundation, Sherman Fairchild Foundation, Schott Foundation for Public Education, Lincy Foundation, Rainwater Charitable Foundation, Robert Galvin, and Mary Jane Brinton. J.S. was supported by a fellowship from the John Douglas French Alzheimer's Foundation and J.C.W. by a fellowship from the Canadian Institutes of Health Research.

1. Hardy J, Selkoe DJ (2002) The amyloid hypothesis of Alzheimer's disease: Progress and problems on the road to therapeutics. *Science* 297:353–356.
2. Braak H, Braak E (1991) Neuropathological stageing of Alzheimer-related changes. *Acta Neuropathol* 82:239–259.
3. Games D, et al. (1995) Alzheimer-type neuropathology in transgenic mice overexpressing V717F β-amyloid precursor protein. *Nature* 373:523–527.
4. Hsiao K, et al. (1996) Correlative memory deficits, Abeta elevation, and amyloid plaques in transgenic mice. *Science* 274:99–102.
5. Sturchler-Pierrat C, et al. (1997) Two amyloid precursor protein transgenic mouse models with Alzheimer disease-like pathology. *Proc Natl Acad Sci USA* 94:13287–13292.
6. Chishti MA, et al. (2001) Early-onset amyloid deposition and cognitive deficits in transgenic mice expressing a double mutant form of amyloid precursor protein 695. *J Biol Chem* 276:21562–21570.
7. Kane MD, et al. (2000) Evidence for seeding of beta-amyloid by intracerebral infusion of Alzheimer brain extracts in beta-amyloid precursor protein-transgenic mice. *J Neurosci* 20:3606–3611.
8. Meyer-Luehmann M, et al. (2006) Exogenous induction of cerebral beta-amyloidogenesis is governed by agent and host. *Science* 313:1781–1784.
9. Eisele YS, et al. (2009) Induction of cerebral β-amyloidosis: intracerebral versus systemic Abeta inoculation. *Proc Natl Acad Sci USA* 106:12926–12931.
10. Watts JC, et al. (2011) Bioluminescence imaging of Abeta deposition in bigenic mouse models of Alzheimer's disease. *Proc Natl Acad Sci USA* 108:2528–2533.
11. Morales R, Duran-Aniotz C, Castilla J, Estrada LD, Soto C (2011) *De novo* induction of amyloid-β deposition *in vivo*. *Mol Psychiatry*, 10.1038/mp.2011.120.
12. Rosen RF, et al. (2012) Exogenous seeding of cerebral β-amyloid deposition in βAPP-transgenic rats. *J Neurochem* 120:660–666.
13. Colby DW, Prusiner SB (2011) Prions. *Cold Spring Harb Perspect Biol* 3:a006833.
14. Wickner RB (1994) [URE3] as an altered URE2 protein: Evidence for a prion analog in *Saccharomyces cerevisiae*. *Science* 264:566–569.
15. Coustou V, Deleu C, Saupe S, Begueret J (1997) The protein product of the *het-s* heterokaryon incompatibility gene of the fungus *Podospora anserina* behaves as a prion analog. *Proc Natl Acad Sci USA* 94:9773–9778.
16. Si K, Choi YB, White-Grindley E, Majumdar A, Kandel ER (2010) Aplysia CPEB can form prion-like multimers in sensory neurons that contribute to long-term facilitation. *Cell* 140:421–435.
17. Hou F, et al. (2011) MAVS forms functional prion-like aggregates to activate and propagate antiviral innate immune response. *Cell* 146:448–461.
18. Aguzzi A, Rajendran L (2009) The transcellular spread of cytosolic amyloids, prions, and prionoids. *Neuron* 64:783–790.
19. Kaneko K, et al. (2000) A synthetic peptide initiates Gerstmann-Sträussler-Scheinker (GSS) disease in transgenic mice. *J Mol Biol* 295:997–1007.
20. Sparrer HE, Santoso A, Szoka FC, Jr., Weissman JS (2000) Evidence for the prion hypothesis: Induction of the yeast [*PSI*$^+$] factor by in vitro-converted Sup35 protein. *Science* 289:595–599.
21. Maddelein ML, Dos Reis S, Duvezin-Caubet S, Coulary-Salin B, Saupe SJ (2002) Amyloid aggregates of the HET-s prion protein are infectious. *Proc Natl Acad Sci USA* 99:7402–7407.
22. Legname G, et al. (2004) Synthetic mammalian prions. *Science* 305:673–676.
23. Zhu L, et al. (2004) Non-invasive imaging of GFAP expression after neuronal damage in mice. *Neurosci Lett* 367:210–212.
24. Hamaguchi T, et al. (2012) The presence of Aβ seeds, and not age per se, is critical to the initiation of Aβ deposition in the brain. *Acta Neuropathol* 123:31–37.
25. Sim VL, Caughey B (2009) Ultrastructures and strain comparison of under-glycosylated scrapie prion fibrils. *Neurobiol Aging* 30:2031–2042.
26. O'Nuallain B, et al. (2010) Amyloid β-protein dimers rapidly form stable synaptotoxic protofibrils. *J Neurosci* 30:14411–14419.
27. Shankar GM, et al. (2008) Amyloid-beta protein dimers isolated directly from Alzheimer's brains impair synaptic plasticity and memory. *Nat Med* 14:837–842.
28. Tamgüney G, et al. (2009) Measuring prions by bioluminescence imaging. *Proc Natl Acad Sci USA* 106:15002–15006.
29. Prusiner SB, et al. (1982) Measurement of the scrapie agent using an incubation time interval assay. *Ann Neurol* 11:353–358.
30. Langer F, et al. (2011) Soluble Aβ seeds are potent inducers of cerebral β-amyloid deposition. *J Neurosci* 31:14488–14495.
31. Wille H, et al. (2009) Natural and synthetic prion structure from X-ray fiber diffraction. *Proc Natl Acad Sci USA* 106:16990–16995.
32. Colby DW, et al. (2009) Design and construction of diverse mammalian prion strains. *Proc Natl Acad Sci USA* 106:20417–20422.
33. Petkova AT, et al. (2005) Self-propagating, molecular-level polymorphism in Alzheimer's beta-amyloid fibrils. *Science* 307:262–265.
34. Kodali R, Williams AD, Chemuru S, Wetzel R (2010) Abeta(1-40) forms five distinct amyloid structures whose β-sheet contents and fibril stabilities are correlated. *J Mol Biol* 401:503–517.
35. Paravastu AK, Qahwash I, Leapman RD, Meredith SC, Tycko R (2009) Seeded growth of beta-amyloid fibrils from Alzheimer's brain-derived fibrils produces a distinct fibril structure. *Proc Natl Acad Sci USA* 106:7443–7448.
36. Lührs T, et al. (2005) 3D structure of Alzheimer's amyloid-beta(1-42) fibrils. *Proc Natl Acad Sci USA* 102:17342–17347.
37. Cairns HJF (1950) Intracerebral inoculation of mice; fate of the inoculum. *Nature* 166:910–911.
38. Safar JG, et al. (2005) Search for a prion-specific nucleic acid. *J Virol* 79:10796–10806.
39. Harris JA, et al. (2010) Transsynaptic progression of amyloid-β-induced neuronal dysfunction within the entorhinal-hippocampal network. *Neuron* 68:428–441.
40. Braak H, Del Tredici K (2011) Alzheimer's pathogenesis: is there neuron-to-neuron propagation? *Acta Neuropathol* 121:589–595.
41. Mougenot AL, et al. (2011) Prion-like acceleration of a synucleinopathy in a transgenic mouse model. *Neurobiol Aging*, 10.1016/j.neurobiolaging.2011.06.022.
42. Volpicelli-Daley LA, et al. (2011) Exogenous α-synuclein fibrils induce Lewy body pathology leading to synaptic dysfunction and neuron death. *Neuron* 72:57–71.
43. Clavaguera F, et al. (2009) Transmission and spreading of tauopathy in transgenic mouse brain. *Nat Cell Biol* 11:909–913.
44. Frost B, Jacks RL, Diamond MI (2009) Propagation of tau misfolding from the outside to the inside of a cell. *J Biol Chem* 284:12845–12852.
45. Guo JL, Lee VM-Y (2011) Seeding of normal Tau by pathological Tau conformers drives pathogenesis of Alzheimer-like tangles. *J Biol Chem* 286:15317–15331.
46. Münch C, O'Brien J, Bertolotti A (2011) Prion-like propagation of mutant superoxide dismutase-1 misfolding in neuronal cells. *Proc Natl Acad Sci USA* 108:3548–3553.
47. Grad LI, et al. (2011) Intermolecular transmission of superoxide dismutase 1 misfolding in living cells. *Proc Natl Acad Sci USA* 108:16398–16403.
48. Eisele YS, et al. (2010) Peripherally applied Abeta-containing inoculates induce cerebral beta-amyloidosis. *Science* 330:980–982.
49. Schenk D, et al. (1999) Immunization with amyloid-beta attenuates Alzheimer-disease-like pathology in the PDAPP mouse. *Nature* 400:173–177.
50. Janus C, et al. (2000) A β peptide immunization reduces behavioural impairment and plaques in a model of Alzheimer's disease. *Nature* 408:979–982.
51. Orgogozo JM, et al. (2003) Subacute meningoencephalitis in a subset of patients with AD after Abeta42 immunization. *Neurology* 61:46–54.
52. Gilman S, et al.; AN1792(QS-21)-201 Study Team (2005) Clinical effects of Abeta immunization (AN1792) in patients with AD in an interrupted trial. *Neurology* 64:1553–1562.